Available online at www.sciencedirect.com
SCIENCE DIRECT®
Carbohydrate Research 340 (2005) 1175–1184
Carbohydrate RESEARCH

Crystal structure and solid state ^{13}C NMR analysis of nitrophenyl 2,3,4,6-tetra-*O*-acetyl-β-D-gluco- and D-galactopyranosides

Andrzej Temeriusz,[a,*] Tomasz Gubica,[a] Paulina Rogowska,[a] Katarzyna Paradowska[b] and Michał K. Cyrański[a]

[a]*Department of Chemistry, Warsaw University, Pasteura 1, Warszawa 02-093, Poland*
[b]*Department of Physical Chemistry, Faculty of Pharmacy, Medical Academy, Banacha 1, 02-097 Warszawa, Poland*

Received 25 November 2004; accepted 15 February 2005

Abstract—The X-ray diffraction analysis of *o*-nitrophenyl 2,3,4,6-tetra-*O*-acetyl-β-D-galactopyranoside (**1**), *m*-nitrophenyl 2,3,4,6-tetra-*O*-acetyl-β-D-galactopyranoside, *p*-nitrophenyl 2,3,4,6-tetra-*O*-acetyl-β-D-galactopyranoside and *o*-nitrophenyl 2,3,4,6-tetra-*O*-acetyl-β-D-glucopyranoside was performed. It was found that except in the case of **1**, all other crystals have one molecule in the independent part of the crystal unit cell. The results support the opinion that the nitro group does not conjugate effectively with the phenyl ring. In the ^{13}C CP MAS spectrum of **1** the signals are split, confirming the presence of two independent molecules. Similarly, the ^{13}C CP MAS NMR spectrum of *p*-nitrophenyl-2,3,4,6-tetra-*O*-acetyl-β-D-glucopyranoside indicated the presence of two non-equivalent molecules in the crystal unit. One of these molecules has more conformational freedom enabling rotation of the phenyl ring.

Keywords: Crystal structure; ^{13}C NMR analysis; Solid-state NMR; Glycosidase; Chemoenzymatic synthesis; Cholera toxin

1. Introduction

Chromogenic properties of the free aglycon of nitrophenyl *O*-glycosides are useful in enzyme studies. For example, *p*-nitrophenyl α-D-galactopyranoside was used by Wakabayashi and Nishizawa[1] in enzymatic investigations on an α-D-galactosidase from bottom yeast fermentary. Sheridan and Brenchley[2] have isolated a characteristic salt-tolerant family of 42 β-galactosidases from the psychrophilic bacterium Gram-positive Antarctic *Planococcus*. Enzyme activity is determined spectrophotometrically based on the release of *p*-nitrophenol from suitable *p*-nitrophenyl-derivative substrates. On the other hand, *p*-nitrophenyl α-D-glucopyranoside was used in studies on the synthetic reactions of two purified enzymes having α-D-glucosidase activities.[3] Hansson et al.[4] determined the activities of the enzymes using *p*-nitrophenyl β-D-glucopyranoside and *p*-nitrophenyl β-D-galactopyranoside as the substrates. Nitrophenyl β-D-glycopyranosides were found to be effective glycosyl donors for the enzymatic β-glycosidation of primary alcohols.[5] Also Rydon and co-workers[6,7] studied the mechanism of acid hydrolysis of *o*-, *m*-, *p*-nitrophenyl β-D-glucopyranosides and *m*-, *p*-nitrophenyl-α-D-glucopyranosides. They found that *ortho* substituted derivatives are hydrolyzed faster than is predicted by the substitution constant. Biosynthesis of the α-D-glucoside of *o*-aminophenol, and probably *p*-nitrophenol, has been demonstrated by Dutton.[8] Moreover, 3,5-substituted nitrophenyl galactosides are potential cholera toxin antagonists.[9] Since biological activity and reaction with enzymes is closely related to molecular structure, the compounds with different positions of nitro substituents to aromatic ring were of interest. Thus

* Corresponding author. Fax: +48 22 822 5996; e-mail: atemer@chem.uw.edu.pl

0008-6215/$ - see front matter © 2005 Elsevier Ltd. All rights reserved.
doi:10.1016/j.carres.2005.02.010

nitrophenyl galactosides and glucosides were studied by means of X-ray diffraction and NMR spectroscopy.

2. Results and discussion

The nitrophenyl glycosides shown in Scheme 1 were prepared by the reaction of the corresponding *per*-acetyl-α-D-bromide with *o*-, *m*- or *p*-nitrophenol according to the described procedures.[10–13] Suitable crystals of *o*-nitrophenyl 2,3,4,6-tetra-*O*-acetyl-β-D-galactopyranoside (**1**), *m*-nitrophenyl 2,3,4,6-tetra-*O*-acetyl-β-D-galactopyranoside (**2**), *p*-nitrophenyl 2,3,4,6-tetra-*O*-acetyl-β-D-galactopyranoside (**3**) and *o*-nitrophenyl 2,3,4,6-tetra-*O*-acetyl-β-D-glucopyranoside (**4**) were obtained by slow crystallization from ethanol. The crystal structures of the four molecules (**1**–**4**) were determined in order to ascertain their stereochemistry and solid state conformations. These data constituted a basis for solid state NMR studies. The configuration, conformation and atom numbering are shown in Figures 1 and 2. Crystal data and structural refinement are specified in Table 1.

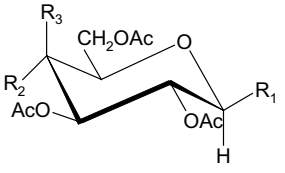

1	R_1 = *O*-(2-NO_2)Ph,	R_2 = H,	R_3 = OAc
2	R_1 = *O*-(3-NO_2)Ph,	R_2 = H,	R_3 = OAc
3	R_1 = *O*-(4-NO_2)Ph,	R_2 = H,	R_3 = OAc
4	R_1 = *O*-(2-NO_2)Ph,	R_2 = OAc,	R_3 = H
5	R_1 = *O*-(3-NO_2)Ph,	R_2 = OAc,	R_3 = H
6	R_1 = *O*-(4-NO_2)Ph,	R_2 = OAc,	R_3 = H

Scheme 1.

Selected bond lengths, bond angles and major torsion angles for **1**–**4** are given in Tables 2–4. Similar to the *o*-nitrophenyl 2,3,4,6-tetra-*O*-acetyl-β-D-glucopyranoside[14] the analyzed galactopyranosides (**1**–**3**) and glucopyranoside (**4**) crystallized in the $P2_1$ space group. Due to sharp deviations of the Flack parameter[15] the absolute configurations could not be determined. Instead, they were assigned based on the knowledge of stereochemistry of the synthetic precursors and the mechanisms of the synthesis. Except in the case of *o*-nitrophenyl 2,3,4,6-tetra-*O*-acetyl-β-D-galactopyranoside (**1**), all other crystals have one molecule in the independent part of the crystal unit cell. In both molecules of *o*-nitrophenyl 2,3,4,6-tetra-*O*-acetyl-β-D-galactopyranoside (**1A** and **1B**) the nitro groups are significantly rotated with respect to the phenyl fragment. The angle between the best planes of the phenyl ring and the nitro group was −61.0° and 53.9° for molecules **1A** and **1B**, respectively (Table 4), and the rotation proceeds in two directions. The extent of distortion from planarity of the nitrobenzene fragment was comparable to that observed in *o*-nitrophenyl 2,3,4,6-tetra-*O*-acetyl-β-D-glucopyranoside (**4**) where the angle is equal to −45.5°. Evidently, in both cases **1** and **4** the gross distortions from planarity result from the steric interactions between the nitro-fragment and sugar moiety. The ab initio optimization (at B3LYP/6-311+G** level of theory) of *o*-methoxynitrobenzene[16] revealed that in the optimal geometry the nitro-group is distorted by 55.5°, and the difference in energy between this structure and the planar one is a mere 1.2 Kcal/mol. This finding supports the earlier opinion[17] that the nitro group does not conjugate effectively with the benzene ring, and can also be well exemplified by the geometries of *p*-nitrophenyl 2,3,4,6-tetra-*O*-acetyl-β-D-galactopyranoside (**3**) and *m*-nitrophenyl 2,3,4,6-tetra-*O*-acetyl-β-D-galactopyranoside (**2**), where due to weak intermolecular interactions

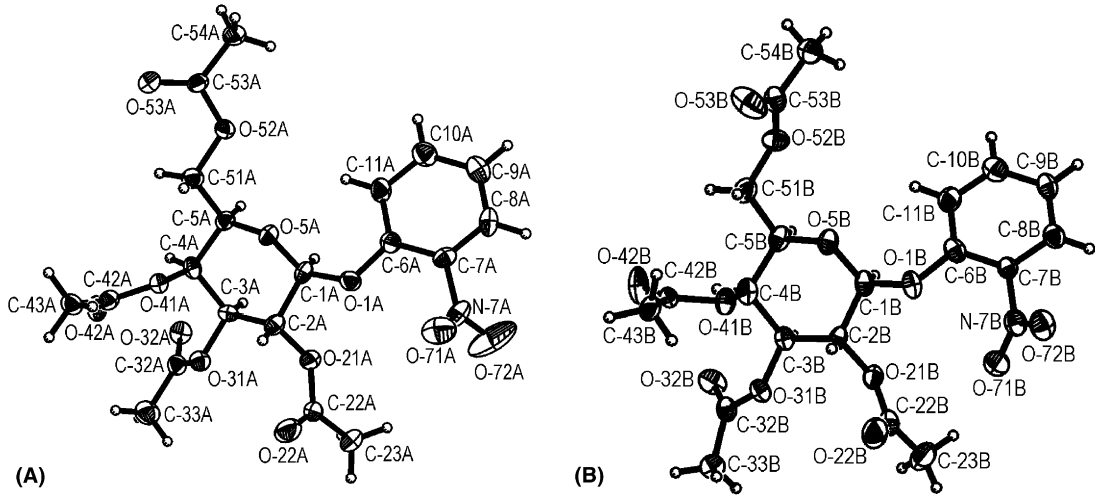

Figure 1. ORTEP and atomic numbering of **1**: *o*-nitrophenyl 2,3,4,6-tetra-*O*-acetyl-β-D-galactopyranoside.

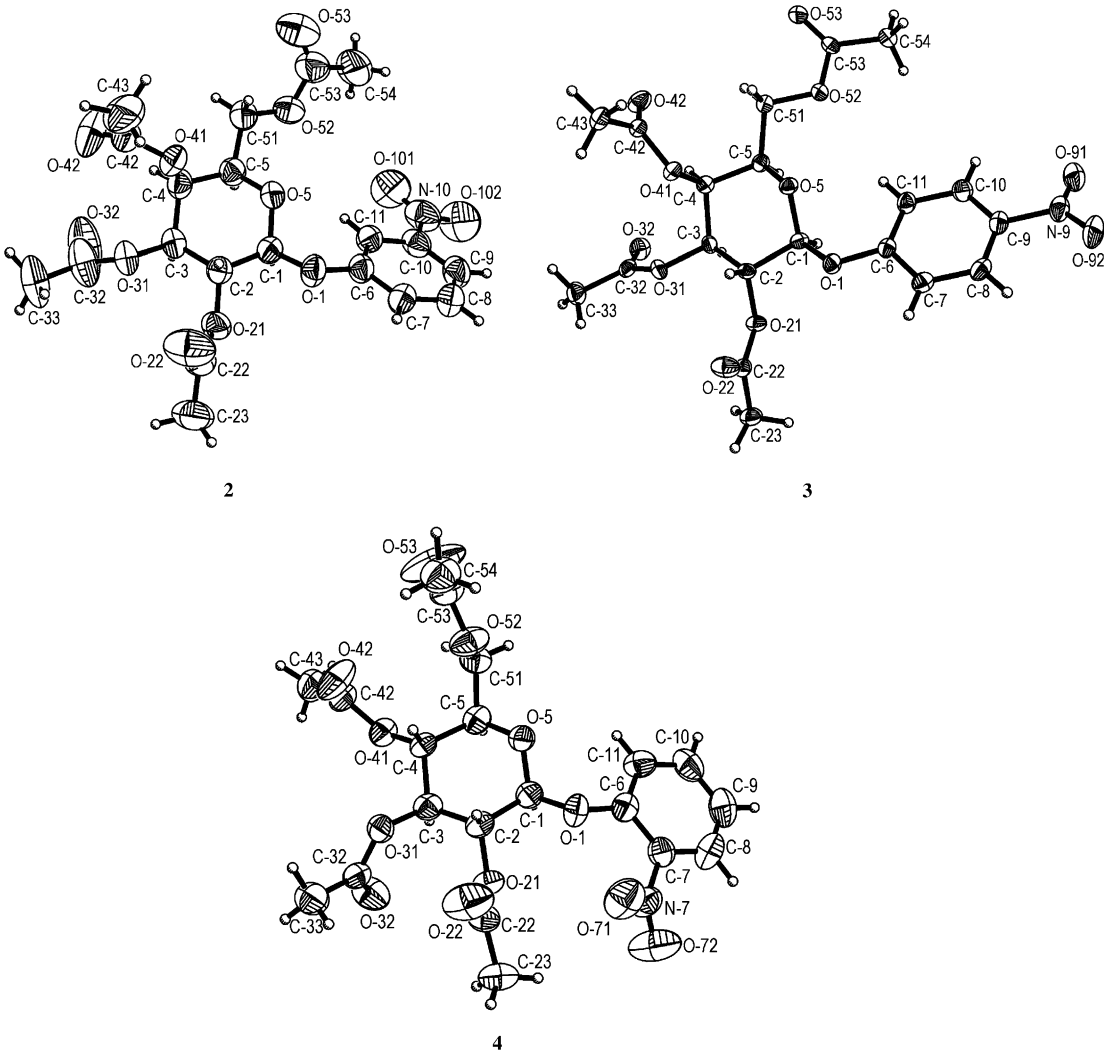

Figure 2. ORTEP and atomic numbering of **2**: *m*-nitrophenyl 2,3,4,6-tetra-*O*-acetyl-β-D-galactopyranoside; **3**: *p*-nitophenyl 2,3,4,6-tetra-*O*-acetyl-β-D-galactopyranoside; **4**: *o*-nitrophenyl 2,3,4,6,-tetra-*O*-acetyl-β-D-glucopyranoside. The ellipsoids are drawn at the 50% probability level.

in the crystal lattice, the nitro group is rotated by −14.2° and 6.1°, respectively.

The most significant difference resulting from different packing forces between two molecules of *o*-nitrophenyl 2,3,4,6-tetra-*O*-acetyl-β-D-galactopyranoside (**1**) involve the torsion angles of the C-5 and C-4 acetyl groups. The C-3–C-4–O-41–C-42, C-5–C-4–O-41–C-42 and C-5–C-51–O-52–C-53 torsion angles are equal to −96.5(5), 142.3(4), 165.8(4) and −129.3(4), 111.6(5), −139.0(5) degrees for molecules **A** and **B**, respectively. Comparison of *o*-nitrophenyl 2,3,4,6-tetra-*O*-acetyl-β-D-galactopyranoside (**1**) with *o*-nitrophenyl 2,3,4,6-tetra-*O*-acetyl-β-D-glucopyranoside (**4**) indicates that, apart from the obvious differences between torsion angles on C-4, the changes involve the torsion angles of the acetyl group on C-3 and C-5. The torsion angles C-2–C-3–O-31–C-32 and C-4–C-3–O-31–C-32 are in the range −149.9(4) and −154.3(4), 84.3(5) and 82.5(5), respectively, for two molecules of *o*-nitrophenyl 2,3,4,6-tetra-*O*-acetyl-β-D-galactopyranoside (**1**) and −99.6(6), 141.2(5), for *o*-nitrophenyl 2,3,4,6-tetra-*O*-acetyl-β-D-glucopyranoside (**4**). Similarly, the torsion angles C-4–C-5–C-51–O-52 and O-5–C-5–C-51–O-52 are in the range −165.2(4) and −171.9(4), 72.4(5) and 66.0(5), respectively, for two molecules of *o*-nitrophenyl 2,3,4,6-tetra-*O*-acetyl-β-D-galactopyranoside (**1**) and 61.0(6), −58.7(6), for *o*-nitrophenyl 2,3,4,6-tetra-*O*-acetyl-β-D-glucopyranoside (**4**). In the case of *p*-nitrophenyl 2,3,4,6-tetra-*O*-acetyl-β-D-galactopyranoside (**3**) and its glucopyranoside analogue (**6**)[14] the most significant difference concerns only the acetyl group on C-3. The torsion angles C-2–C-3–O-31–C-32 and C-4–C-3–O-31–C-32. They are equal to −155.7(2), 80.9(2) and, –112.7, 126.9, respectively, for *p*-nitrophenyl 2,3,4,6-tetra-*O*-acetyl-β-D-galactopyranoside (**3**) and *p*-nitrophenyl 2,3,4,6-tetra-*O*-acetyl-β-D-glucopyranoside (**6**).[14]

The sugar moieties adopt $^4C_1$ conformations, however, due to crystal packing forces they are always

Table 1. Crystal data and structure refinement for *o*-nitrophenyl 2,3,4,6-tetra-*O*-acetyl-β-D-galactopyranoside (**1**) *m*-nitrophenyl 2,3,4,6-tetra-*O*-acetyl-β-D-galactopyranoside (**2**) *p*-nitrophenyl 2,3,4,6-tetra-*O*-acetyl-β-D-galactopyranoside (**3**) and *o*-nitrophenyl 2,3,4,6-tetra-*O*-acetyl-β-D-glucopyranoside (**4**)

Compound	**1**	**2**	**3**	**4**
Empirical formula	$2C_{20}H_{23}NO_{12}$	$C_{20}H_{23}NO_{12}$	$C_{20}H_{23}NO_{12}$	$C_{20}H_{23}NO_{12}$
Formula weight	938.79	469.39	469.39	469.39
Temperature (K)	110(2)	293(2)	130(2)	293(2)
Space group	$P2_1$	$P2_1$	$P2_1$	$P2_1$
Unit cell dimensions				
a (Å)	11.388(2)	10.210(2)	11.758(2)	10.711(2)
b (Å)	8.188(2)	8.435(2)	5.715(2)	8.276(2)
c (Å)	23.867(5)	13.577(3)	17.379(3)	12.792(3)
β (°)	103.44(3)	102.50(3)	109.65(3)	102.80(3)
Volume (Å^3)	2164.5(7)	1141.6(4)	1099.8(4)	1105.8(4)
Z (molecules/cell)	2	2	2	2
$D_{calculated}$ (Mg/m^3)	1.440	1.366	1.417	1.410
Absorption coefficient (mm^{-1})	0.121	0.115	0.119	0.118
F (000)	984	492	492	492
Crystal size (mm)	$0.3 \times 0.2 \times 0.2$	$0.4 \times 0.3 \times 0.2$	$0.4 \times 0.3 \times 0.1$	$0.1 \times 0.05 \times 0.05$
Θ range for data collection (°)	3.33–25.0	3.71–22.49	3.57–24.99	2.81–22.49
Limiting indices	$-13 \leqslant h \leqslant 13$, $-7 \leqslant k \leqslant 9$ $-28 \leqslant l \leqslant 28$	$-10 \leqslant h \leqslant 10$, $-8 \leqslant k \leqslant 9$ $-14 \leqslant l \leqslant 14$	$-13 \leqslant h \leqslant 13$, $-6 \leqslant k \leqslant 4$ $-20 \leqslant l \leqslant 20$	$-11 \leqslant h \leqslant 11$ $-8 \leqslant k \leqslant 8$ $-11 \leqslant l \leqslant 13$
Reflections collected	16,282	6863	7971	6272
Independent reflections	5769 [R_{int} = 0.0675]	2467 [R_{int} = 0.0259]	2772 [R_{int} = 0.0299]	2816 [R_{int} = .0950]
Refinement method	Full-matrix Least-squares on F^2	Full-matrix Least-squares on F^2	Full-matrix Least-squares on F^2	Full-matrix Least-squares on F^2
Data (restraints) parameters	5768/1/604	2467/1/303	2772/1/303	2816/1/303
Goodness-of-fit on F^2	1.004	1.010	1.057	0.975
Final R indices [$I > 2\sigma(I)$]	R_1 = 0.0596, wR_2 = 0.1220	R_1 = 0.0460, wR_2 = 0.1212	R_1 = 0.0307, wR_2 = 0.0780	R_1 = 0.0635, wR_2 = 0.1490
R indices (all data)	R_1 = 0.0937, wR_2 = 0.1427	R_1 = 0.0533, wR_2 = 0.1294	R_1 = 0.0333, wR_2 = 0.0801	R_1 = 0.0933, wR_2 = 0.1824
Extinction coefficient	0.004(1)	0.023(6)	0.016(3)	0.028(5)
Largest difference peak and hole (e/Å^3)	0.598 and −0.314	0.320 and −0.211	0.161 and −0.179	0.224 and −0.222

Table 2. Selected bond lengths (Å) for *o*-nitrophenyl 2,3,4,6-tetra-*O*-acetyl-β-D-galactopyranoside (**1**) *m*-nitrophenyl 2,3,4,6-tetra-*O*-acetyl-β-D-galactopyranoside (**2**) *p*-nitrophenyl 2,3,4,6-tetra-*O*-acetyl-β-D-galactopyranoside (**3**) and *o*-nitrophenyl 2,3,4,6-tetra-*O*-acetyl-β-D-glucopyranoside (**4**)

Atoms	Compound				
	1A	**1B**	**2**	**3**	**4**
C-1–O-5	1.395(6)	1.417(6)	1.409(4)	1.416(2)	1.402(7)
C-1–O-1	1.409(5)	1.414(6)	1.407(4)	1.402(2)	1.383(7)
C-1–C-2	1.508(7)	1.495(7)	1.519(5)	1.510(3)	1.544(9)
O-1–C-6	1.364(6)	1.378(6)	1.381(4)	1.378(2)	1.360(7)
C-2–C-3	1.506(6)	1.512(7)	1.528(5)	1.516(3)	1.524(9)
C-3–C-4	1.532(6)	1.508(7)	1.529(5)	1.535(3)	1.521(9)
C-4–C-5	1.503(7)	1.513(7)	1.513(5)	1.516(3)	1.558(9)
C-5–O-5	1.442(6)	1.431(6)	1.432(4)	1.439(2)	1.432(7)
C-5–C-51	1.488(7)	1.501(7)	1.508(5)	1.501(3)	1.499(9)
C-7–N-7	1.471(7)	1.462(7)			1.447(10)
N-7–O-71	1.188(7)	1.217(6)			1.207(8)
N-7–O-72	1.208(7)	1.229(6)			1.202(8)
C-8–N-8			1.470(6)		
N-8–O-81			1.215(5)		
N-8–O-82			1.217(5)		
C-9–N-9				1.470(3)	
N-9–O-91				1.223(3)	
N-9–O-92				1.224(3)	

slightly distorted. The most significant deviations are found for compound (**3**), as quantified by the Cremer–Pople Θ puckering parameters.[18] The Θ is equal to 12.5°, while the other puckering parameters Q and φ are equal to 0.584 and 350.69. For comparison the Θ is equal to 10.8°, 6.9°, 5.2° and 5.9°, respectively, for two independent molecules of (**1**), as well as for (**2**) and (**4**), while the Q and φ are equal to 0.575 and 50.77 and 0.536 and 20.21, respectively, for two molecules of (**1**), 0.576 and 2.05 for (**2**), 0.582 and 40.72 for (**4**). For an ideal chair conformation $^4C_1$ the Θ angle is equal to 0°. Figure 3 shows as an example the intermolecular interactions in the crystal lattice of $P1$. The attempts to grow a suitable single crystal of **5** were unsuccessful, and solid state structure of **6** was known from previous XRD studies.[14]

The one- and two-dimensional ^{1}H and ^{13}C NMR spectra for $CDCl_3$ solutions of **1**–**6** were recorded and analyzed in order to achieve a reliable assignment of ^{13}C resonances. The spectra for solids were recorded using the cross-polarization (CP) magic angle spinning (MAS) technique and the ^{13}C CP MAS NMR spectra

Table 3. Selected bond angles (°) for *o*-nitrophenyl 2,3,4,6-tetra-*O*-acetyl-β-D-galactopyranoside (**1**) *m*-nitrophenyl 2,3,4,6-tetra-*O*-acetyl-β-D-galactopyranoside (**2**) *p*-nitrophenyl 2,3,4,6-tetra-*O*-acetyl-β-D-galactopyranoside (**3**) and *o*-nitrophenyl 2,3,4,6-tetra-*O*-acetyl-β-D-glucopyranoside (**4**)

Atoms	Compound				
	1A	**1B**	**2**	**3**	**4**
O-1–C-1–O-5	108.8(4)	107.6(4)	107.1(3)	108.2(2)	109.1(5)
O-5–C-1–C-2	108.8(4)	109.6(4)	110.1(3)	108.1(2)	108.2(5)
O-1–C-1–C-2	109.1(4)	106.6(4)	107.9(3)	108.2(2)	106.1(5)
C-6–O-1–C-1	116.0(4)	117.7(4)	117.9(3)	117.9(2)	118.8(5)
O-31–C-3–C-4	112.0(4)	112.8(4)	110.8(3)	110.9(2)	108.0(5)
C-2–C-3–C-4	113.3(4)	112.3(4)	112.1(3)	113.7(2)	110.5(5)
O-41–C-4–C-5	108.6(4)	109.2(4)	109.6(3)	111.6(2)	107.4(5)
O-41–C-4–C-3	111.1(4)	108.1(4)	109.8(3)	108.3(2)	108.4(4)
C-5–C-4–C-3	110.1(4)	109.5(4)	109.0(3)	107.8(2)	111.0(5)
C-42–O-41–C-4	115.9(4)	116.9(4)	119.0(4)	117.1(2)	117.8(5)
O-5–C-5–C-4	111.3(4)	111.5(4)	110.1(3)	109.7(2)	108.9(5)
C-51–C-5–C-4	112.2(4)	111.1(4)	112.6(3)	115.5(2)	111.6(5)

Table 4. Selected torsion angles for *o*-nitrophenyl 2,3,4,6-tetra-*O*-acetyl-β-D-galactopyranoside (**1**) *m*-nitrophenyl 2,3,4,6-tetra-*O*-acetyl-β-D-galactopyranoside (**2**) *p*-nitrophenyl 2,3,4,6-tetra-*O*-acetyl-β-D-galactopyranoside (**3**) and *o*-nitrophenyl 2,3,4,6-tetra-*O*-acetyl-β-D-glucopyranoside (**4**)

Torsion angle	Compound				
	1A	**1B**	**2**	**3**	**4**
O-5–C-1–O-1–C-6	−82.0(5)	−89.2(5)	−77.1(4)	−73.6(2)	−86.9(6)
C-2–C-1–O-1–C-6	159.5(4)	153.2(4)	164.3(3)	169.6(2)	156.8(5)
O-1–C-1–C-2–O-21	−62.5(5)	−68.1(5)	−70.2(4)	−71.0(2)	−62.2(6)
O-5–C-1–C-2–C-3	62.7(5)	57.9(5)	56.7(4)	55.0(2)	59.9(6)
O-1–C-1–C-2–C-3	−178.8(4)	174.1(4)	173.3(3)	171.9(2)	176.8(5)
C-1–O-1–C-6–C-7	−154.7(4)	−152.9(4)	−167.7(4)	−165.10(17)	−134.8(64)
C-2–C-3–O-31–C-32	−149.9(4)	−154.3(4)	−148.0(4)	−155.7(2)	−99.6(6)
C-4–C-3–O-31–C-32	84.3(5)	82.5(5)	89.9(5)	80.9(2)	141.2(5)
C-5–C-4–O-41–C-42	142.3(4)	111.6(5)	138.5(3)	99.3(2)	128.3(6)
C-3–C-4–O-41–C-42	−96.5(5)	−129.3(4)	−101.8(4)	−142.3(2)	−111.7(6)
O-5–C-5–C-51–O-52	72.4(5)	66.0(5)	68.0(4)	65.7(2)	−58.7(6)
C-4–C-5–C-51–O-52	−165.2(4)	−171.9(4)	−171.3(3)	−171.6(2)	61.0(6)
C-5–C-51–O-52–C-53	165.8(4)	−139.0(5)	−165.8(4)	154.4(2)	−156.0(6)
C-4–O-41–C-42–O-42	10.5(7)	−1.2(7)	−3.0(6)	−5.7(3)	−5.2(10)
C-4–O-41–C-42–C-43	−167.2(4)	−179.3(4)	177.1(4)	175.5(2)	173.6(5)
C-6–C-7–N-7–O-71	−61.0(7)	53.9(7)			−45.5(9)
C-6–C-7–N-7–O-72	127.2(6)	−126.8(5)			136.4(7)
C-11–C-10–N-10–O-101			6.1(6)		
C-11–C-10–N-10–O-102			−174.0(5)		
C-8–C-7–N-7–O-71	118.2(6)	−125.6(5)			136.8(7)
C-8–C-7–N-7–O-72	−53.6(7)	53.7(6)			− 41.3(10)
C-8–C-9–N-9–O-91				−14.2(3)	
C-8–C-9–N-9–O-92				166.7(2)	
C-9–C-10–N-10–O-101			−173.6(5)		
C-9–C-10–N-10–O-102			6.2(7)		
C-10–C-9–N-9–O-91				165.9(2)	
C-10–C-9–N-9–O-92				−13.2(3)	

of **2** and **4** are illustrated in Figures 4 and 5, respectively. Chemical shifts were assigned on the basis of liquid-state ones. However, some solid-state resonances had significantly different chemical shifts from their liquid-state counterparts. These resonances were assigned, following the same sequence as the calculated shielding constants. The ^{13}C NMR chemical shifts for glycosides **1**–**3** and **4**–**6**, are collected in Tables 5 and 6, respectively. The differences between solution ($CDCl_3$) and solid state $\Delta = \delta_{solid} - \delta_{solution} > 1$ ppm are given in parentheses. In the spectrum of *o*-nitrophenyl 2,3,4,6-tetra-*O*-acetyl-β-D-galctopyranoside (**1**) the signals in ^{13}C CP MAS are split, confirming the presence of two independent molecules. The most striking differences in chemical shifts between the molecules **1A** and **1B** appear for C-6 (ca. 3 ppm). Remarkable differences in torsional angles: C-5–C-51–O-52–C-53 of 165.8° and −139.0° are shown by XRD (Table 4). The splitting of aromatic carbon

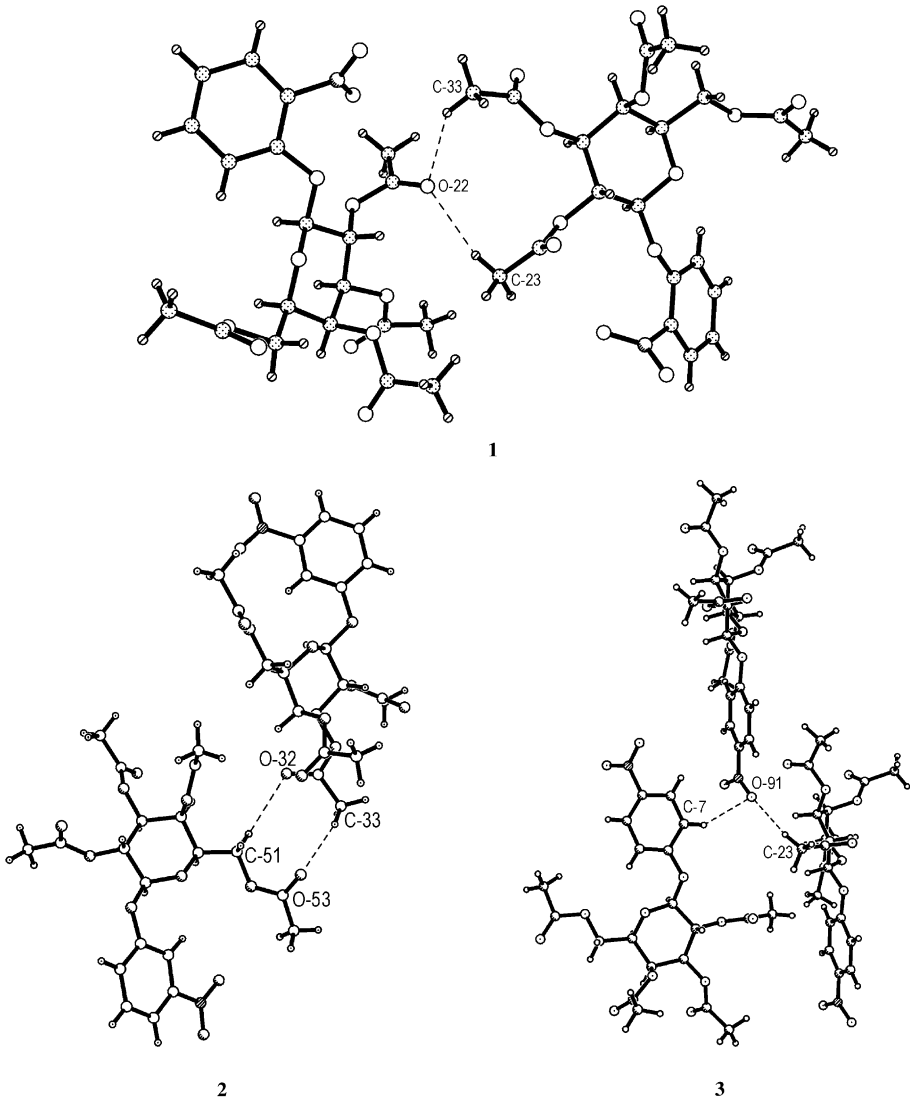

Figure 3. The intermolecular interactions in the crystal lattice of **1**: *o*-nitrophenyl-2,3,4,6-tetra-*O*-acetyl-β-D-galactopyranoside, **2**: *m*-nitrophenyl-2,3,4,6-tetra-*O*-acetyl-β-D-galactopyranoside and **3**: *p*-nitrophenyl-2,3,4,6-tetra-*O*-acetyl-β-D-galactopyranoside.

signals results from twist angles of the ring C-1–O-1–C-6–C-7 of 154.4° in **1A** and 152.8° in **1B**.

Significant Δ values for C-1 and C-6 carbons are observed for all compounds (Table 5), and can be explained by the frozen reorientation around C–O bonds in the solid phase whereas in solution these two moieties are flexible (rotation around glycosidic bonds and CH_2O– group).

As noticed previously,[14] the carbonyl bonds of the acetyl groups on C-2, C-3 and C-4 are nearly coplanar with respective ring C–H bonds and point in the same direction. However, this is not the case for the peracetylated glycosides studied here. Some acetyl substituents were significantly twisted out of the plane, especially C-4–OAc in **3** (C-5–C-4–O-41–C-42, torsional angle 99.3(2)°) and in **1** (C-3–C-4–O-41–C-42, −96.5(5)°). The twisting was reflected in the differences in chemical shifts of the respective sugar carbons (the Δ values of 1–3 ppm).

Generally, liquid-to-solid shifts reflect intramolecular as well as intermolecular interactions.[19] None of the compounds **1**–**6** has a hydrogen bond donor (OH or NH) and there are no strong intermolecular hydrogen bonds; short intermolecular contacts in the crystals consist mainly of CH···O interactions. The differences, Δ, may also result from these intermolecular effects (see the pattern of interactions illustrated in Fig. 3). For example, in the crystal lattice the molecules are linked by CH···O bonds with C···O distances of 3.39 Å in **1**, and 3.54 Å in **3**. Inspection of data from Table 5 indicates that these interactions do not produce significant effects on chemicals shifts (comparing solution and solid-state data for the respective carbons).

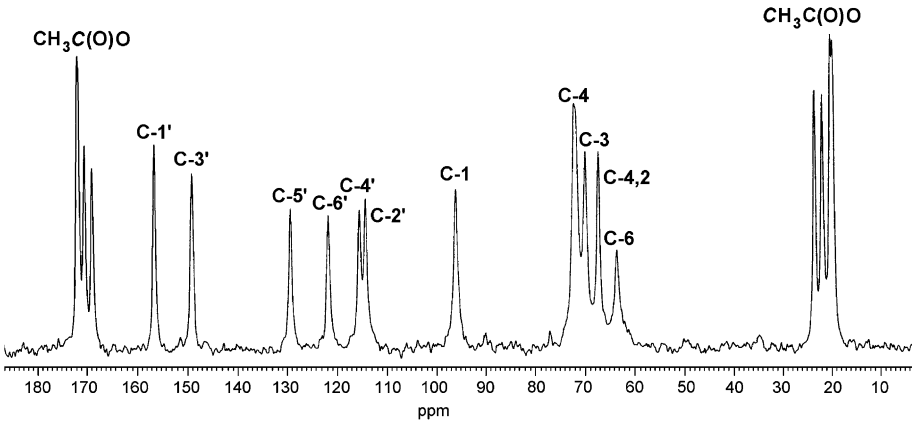

Figure 4. ^{13}C CP MAS spectrum **2**: *m*-nitrophenyl 2,3,4,6-tetra-*O*-acetyl-β-D-galactopyranoside.

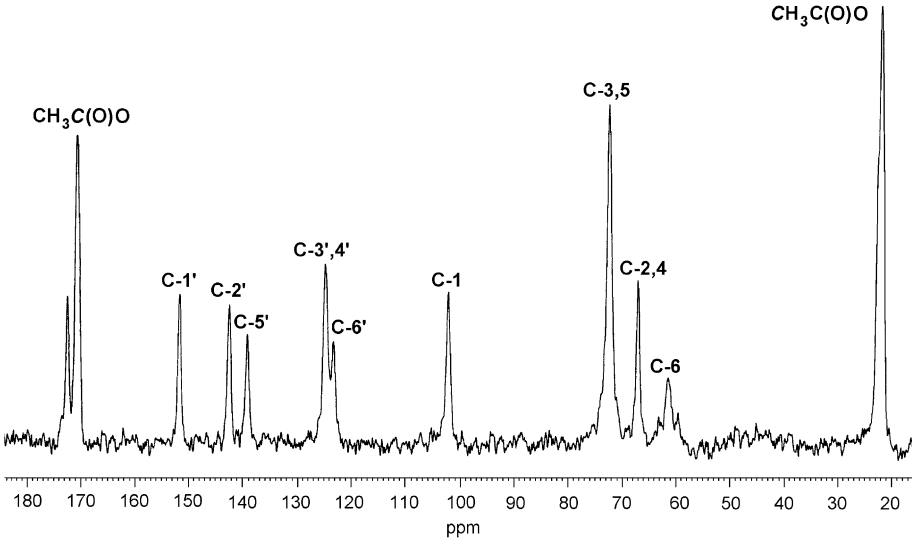

Figure 5. ^{13}C CP MAS spectrum **4**: *o*-nitrophenyl 2,3,4,6-tetra-*O*-acetyl-β-D-glucopyranoside.

An attempt has been made to reproduce and interpret NMR observations using theoretical methods. The calculations were performed for an isolated molecule of glycoside at its equilibrium geometry and not for X-ray geometry (which were determined later).

The isotropic NMR shielding constants calculated by DFT GIAO method for **1**–**6** and correlation of experimental (CP MAS) and theoretical (σ, ppm) parameters are collected in Tables 5 and 6. Reasonable agreement between the experimental (CP MAS) data and theoretical shielding constants were obtained for **2**–**4**, as indicated by the correlation coefficients R^2 0.985–0.99 (see Table 5). Inspection of the final geometries of **1**–**6** showed that acetyl substituents are approximately planar, whereas some of them are twisted in the crystals. These differences in geometry are the source of discrepancies observed when comparing δ and σ values. More striking discrepancies appear for **3** ($R^2 = 0.91$), for which most significant deviations from planarity are observed. Additionally, theoretical shieldings do not reflect any intermolecular interactions.

An interesting effect has been observed in the ^{13}C CP MAS NMR spectra of **6**—the splitting of signals, best observed for the resonances of C-1, C-1′, C-4′ and C-6 (Fig. 6). X-ray data for this compound already existed.[14] The ^{13}C CP MAS NMR spectra of **6** indicated the presence of two non-equivalent molecules in the crystal unit. One of these molecules has more conformational freedom enabling rotation of the phenyl ring, as indicated by the averaged chemical shifts of aromatic carbons (C-2′,6′ 127.6 ppm; C-3′,5′ 117.8 ppm). In the second type of molecules the ring probably has less space and this rotation is frozen (δ C-3′ 121.0 and C-5′ 111.2 ppm, C-6′ 126.5, C-2′ 127.6). A strong effect produced at carbons proximal to nitro substituent may suggest its fast rotation, in addition to the dynamics of aromatic ring.

Table 5. ^{13}C NMR data (δ in ppm) for nitrophenyl 2,3,4,6-tetra-*O*-acetyl-β-D-galactopyranosides (**1**–**3**), the isotropic NMR shielding constants calculated by DFT and correlation of experimental (CPMAS), and theoretical (σ, ppm) parameters

Atom	**1A**,**B**			**2**			**3**		
	δ_{liquid}	δ_{solid}	σ	δ_{liquid}	δ_{solid}	σ	δ_{liquid}	δ_{solid}	σ
C-1	100.8	100.8	96.77	99.30	96.06(−3.2)	83.52	98.57	99.03	
C-2	67.77	69.10(1.3)	73.58	68.50	67.30(−1.2)	68.74	68.28	70.72(2.4)	67.57
C-3	70.56	71.14	68.08	70.78	69.99	61.54	70.58	71.84(1.3)	61.91
C-4	66.73	67.40	67.40	67.14	62.72	60.19	66.72	67.88(1.2)	58.52
C-5	71.39	73.32(2.0)	65.20	71.82	72.21	63.24	71.46	74.73(3.3)	64.77
C-6	61.34	65.90(4.6) **A** 62.83(1.5) **B**	59.28	61.97	63.53(1.6)	69.11	61.37	63.67(2.3)	59.52
C-1′	143.3	149.9(6.6) **A** 149.4(6.0) **B**	150.1	157.2	156.7	154.2	161.2	162.6(1.7)	162.9
C-2′	141.4	142.5(1.0)	138.5	111.4	114.2(2.8)	118.8	125.8	125.8	103.7
C-3′	125.1	125.7	125.9	149.2	149.3	149.7	116.6	116.0	131.8
C-4′	123.8	124.7 **A** 124.0 **B**	123.6	118.3	115.4(−2.9)		143.2	144.2(1.0)	139.6
C-5′	133.7	135.0(1.3)		130.3	129.3(−1.1)	127.2	116.6	119.4(2.8)	132.9
C-6′	119.7	118.0(−1.7) **A** 116.6(−3.1) **B**	120.2	123.9	121.7(−2.2)	117.2	125.8	127.6(−1.8)	115.0
CH_3	20.66, 20.58	23.20, 22.90, 21.69, 20.91	20.97, 20.46, 18.92, 18.67	20.85, 20.76, 20.72, 20.69	23.57, 21.99, 20.27, 19.84	20.64, 20.51, 18.95, 18.79	20.71, 20.67, 20.64, 20.57	21.28, 20.03	22.87, 20.68, 18.97, 18.87
OAc	170.3 170.2 170.1 169.4	173.0, 172.6, 171.7, 170.6	171.7, 171.1, 169.5, 169.3	170.7, 170.3, 170.1, 169.5	171.8, 170.4, 168.9	171.7, 171.0, 170.5, 170.1	170.3, 170.1, 169.3	172.8, 172.4, 170.4	170.9, 170.3, 170.1, 169.1

Table 6. ^{13}C NMR data (δ in ppm) for nitrophenyl 2,3,4,6-tetra-*O*-acetyl-β-D-glucopyranosides (**4**–**6**), the isotropic NMR shielding constants calculated by DFT and correlation of experimental (CPMAS), and theoretical (σ, ppm) parameters

Atom	**4**			**5**			**6A**,**B**		
	δ_{liquid}	δ_{solid}	σ	δ_{liquid}	δ_{solid}	σ	δ_{liquid}	δ_{solid}	σ
C-1	100.1	102.2(2.1)	96.2	98.60	101.0(2.5)	88.42	98.04	96.43(−1.6) **A** 102.42(4.4) **B**	88.85
C-2	68.09	67.14(−1.0)	70.27	68.13	70.35(2.2)	69.64	67.99	70.40(2.4)	69.44
C-3	70.46	72.42(1.0)	69.70	70.95	70.35	70.18	70.91	71.33	69.97
C-4	68.09	67.14(−1.0)	69.58	68.13	70.35(2.2)	69.68	67.99	70.40(2.4)	69.53
C-5	72.30	72.42	66.88	72.46	73.18	67.03	72.42	72.60	67.18
C-6	61.77	61.68	64.49	62.02	64.41(2.4)	64.11	61.81	65.03(3.2) **A** 67.00(5.2) **B**	64.18
C-1′	149.2	151.6(2.4)	151.2	157.0	157.9	154.0	161.2	170.0 **A** 165.0(3.8) **B**	162.9
C-2′	141.2	142.5(1.3)	142.5	111.2	107.4(−3.8)	106.9	125.8	127.6(1.8)	130.8
C-3′	125.2	124.9	126.6	149.1	148.8	147.5	116.6	121.0(4.4) **A** 117.8(1.2) **B**	103.6
C-4′	123.9	124.9(1.0)	124.9	118.2	118.7	118.9	143.2	140.8(−2.4) **A** 144.7(1.5) **B**	140.0
C-5′	133.8	139.2(5.4)	134.0	130.2	132.1(1.9)	129.6	116.6	111.2(−5.4) **A** 117.8(1.2) **B**	115.3
C-6′	119.8	123.4(3.6)	114.6	123.8	124.6	128.5	125.8	126.5 **A** 127.6(1.8) **B**	133.3
CH_3	20.69, 20.60, 20.59, 20.56	21.77	19.23, 19.04, 18.92, 18.90	20.63, 20.59	21.15	19.19, 18.99, 18.85, 18.19	20.68, 20.61, 20.59	22.84, 21.39, 20.69	19.19, 18.98, 18.87, 18.78
OAc	170.5, 170.2, 169.3	172.4, 170.7	170.6, 170.2, 170.1, 169.7	170.7, 170.1, 169.4, 169.2	170.7	170.3, 170.0, 169.4, 169.3	170.4, 170.1, 169.4, 169.2	173.6, 172.9, 171.5, 170.4	170.5, 170.0, 169.4, 169.2

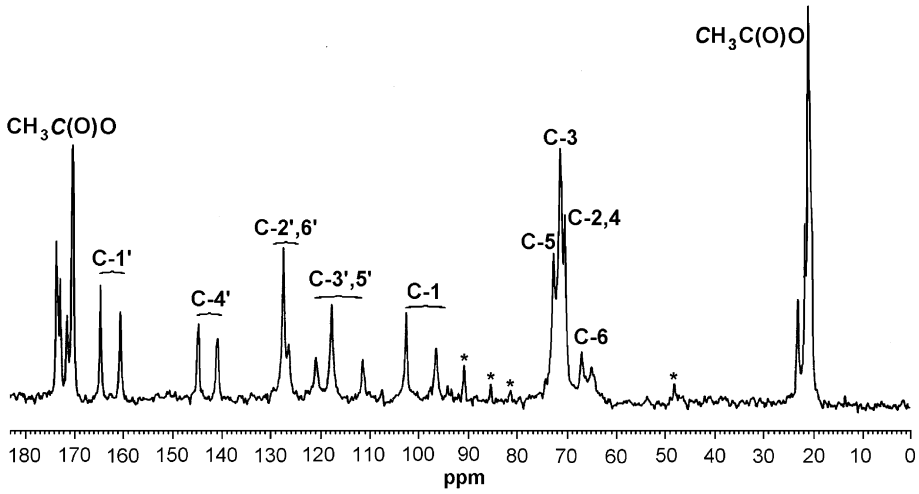

Figure 6. ^{13}C CP MAS spectrum **6**: *p*-nitrophenyl 2,3,4,6-tetra-*O*-acetyl-β-D-glucopyranoside (*, spinning side band).

3. Experimental

3.1. *o*-Nitrophenyl 2,3,4,6-tetra-*O*-acetyl-β-D-galactopyranoside (1)

This compound was prepared according to the procedures described by Seidman and Link.[10] White crystals, yield, 48%; mp 175–176 °C, lit.[10] 172–172.5 °C; $[\alpha]_D^{20}$ +55.4° ($CHCl_3$); $[\alpha]_D^{18}$ +69.9° ($CHCl_3$).

3.2. *m*-Nitrophenyl 2,3,4,6-tetra-*O*-acetyl-β-D-galactopyranoside (2)

This compound was prepared according to the procedures described by Sidhu and co-workers.[11] White crystals, yield, 52%; mp 109–111 °C, $[\alpha]_D^{20}$ −8.1 ($CHCl_3$) lit.[11] 105–106 °C; $[\alpha]_D^{22}$ −8 ($CHCl_3$).

3.3. *p*-Nitrophenyl 2,3,4,6-tetra-*O*-acetyl-β-D-galactopyranoside (3)

This compound was prepared according to the procedures described by Matta and Barlow.[12] White crystals, yield, 49%; mp 146–147 °C, $[\alpha]_D^{20}$ −9.7 ($CHCl_3$), lit.[12] mp 140–142 °C; $[\alpha]_D^{23}$ −11.3 ($CHCl_3$).

3.4. General synthesis of nitrophenyl 2,3,4,6-tetra-*O*-acetyl-β-D-glucopyranoside

A mixture of tetra-*O*-acetyl-α-D-glucopyranosyl bromide (2 mmol), appropriate nitrophenol (4 mmol), silver carbonate (3 mmol) and anhydrous calcium sulfate (Dreirite) in acetonitrile (40 mL) was refluxed for 1 h. After filtration, the mixture was concentrated. The residue was crystallized from ethanol. A solution of the obtained crystals in chloroform was filtered through a layer of silica gel, and washed with chloroform. The combined filtrate and washings were concentrated, and then the residue was crystallized from EtOH to give the desired products.

3.5. *o*-Nitrophenyl 2,3,4,6-tetra-*O*-acetyl-β-D-glucopyranoside (4)

This compound was prepared according to the general procedure. White crystals, yield, 46%; mp 161–162 °C, $[\alpha]_D^{20}$ +40.6 ($CHCl_3$) lit.[13] 157–158 °C; $[\alpha]_D^{22}$ +37 ($CHCl_3$).

3.6. *m*-Nitrophenyl 2,3,4,6-tetra-*O*-acetyl-β-D-glucopyranoside (5)

This compound was prepared according to the general procedure. White crystals, yield, 38%; mp 141–142 °C, $[\alpha]_D^{20}$ −35.7 ($CHCl_3$) lit.[13] 138–139 °C; $[\alpha]_D^{22}$ −40 ($CHCl_3$).

3.7. *p*-Nitrophenyl 2,3,4,6-tetra-*O*-acetyl-β-D-glucopyranoside (6)

This compound was prepared according to the general procedure. White crystals, yield, 30%; mp 177–178.5 °C, $[\alpha]_D^{20}$ −38.6 ($CHCl_3$) lit.[13] 175–177 °C; $[\alpha]_D^{22}$ −27 ($CHCl_3$).

3.8. Physical measurements

X-ray measurements were performed on a Kuma KM4CCD κ-axis diffractometer with graphite-monochromated Mo Kα radiation (0.71073 Å). The crystals of **1** and **3** were measured at 110 and 130 K, respectively, whereas **2** and **4** were measured at 293 K because their crystals were unstable when cooling, (the reason for significantly bigger thermal ellipsoids in their case). The crystals were positioned at 62.3 mm from the KM4CCD camera, 500 frames were measured at 1.2° intervals with

a counting time of 25 s, 600 frames were measured at 1.0° intervals with a counting time of 20 s, 600 frames were measured at 1.0° intervals with a counting time of 10 s, and 748 frames were measured at 0.8 intervals with a counting time of 50 s, respectively. The data were corrected for Lorentz and polarization effects. The numerical absorption correction was not applied. Data reduction and analysis were carried out with the Kuma Diffraction (Wrocław, Poland) programs. The structures were solved by direct methods[20] and refined using SHELXL.[21] The refinement was based on F^2 for all reflections except for those with very negative F^2. The weighted R factor, wR and all goodness-of-fit S values are based on F^2. The non-hydrogen atoms were refined anisotropically, whereas the H-atoms were placed in the calculated positions. Scattering factors were taken from Tables 6.1.1.4 and 4.2.4.2 in Ref. 22.

The ^{13}C NMR spectra were recorded on a Bruker MSL-300 instrument at 75.5 MHz for $CDCl_3$ solution and the solid state. Cross-polarization magic angle spinning (CP MAS) solid state spectra were recorded with spinning speed of 3.4 and 10 kHz, and a contact time of 4 ms. A repetition time of 6 s and a spectral width of 20 kHz were used for accumulation of 400 scans. Chemical shifts were calibrated indirectly through the glycine C=O signal recorded at 176.3 ppm relative to TMS.

4. Supplementary data

Full crystallographic details, except the structure features, have been deposited with the Cambridge Crystallographic Data Centre. These data may be obtained, on request, from The Directory, Cambridge Crystallographic Data Centre, 12 Union Road, Cambridge, CB2 1EZ, UK (fax: +44 1223 336033; e-mail: deposit@ccdc.cam.ac.uk or www: http://www.csdc.cam.ac.uk). Deposition numbers CCDC 256290 (**1**) CCDC 256291 (**2**) CCDC 256292 (**3**) CCDC 256293 (**4**).

Acknowledgements

Financial support from the Warsaw University (BST-831/14/2003) is gratefully acknowledged. The X-ray measurements were undertaken in the Crystallographic Unit of the Physical Chemistry Laboratory at the Chemistry Department of the University of Warsaw.

References

1. Wakabayashi, K.; Nishizawa, K.. *Seigaku* **1955**, *27*, 662–665, *Chem. Abstr*., **1961**, *55*, 1743a.
2. Sheridan, P. P.; Brenchley, J. E. *Appl. Environ. Microbiol.* **2000**, *66*, 2438–2444.
3. Lai, H. L.; Axelrod, B. *Biochim. Biophys. Acta.* **1975**, *391*, 121–128.
4. Hansson, T.; Andersson, M.; Wehtje, E.; Adlercreutz, P. *Enzyme Microb. Technol.* **2001**, *29*, 527–534.
5. Kurashima, K.; Fujii, M.; Ida, Y.; Akita, H. *J. Mol. Catal. B-Enzym.* **2003**, *26*, 87–89.
6. Nath, R. L.; Rydon, H. N. *Biochem. J.* **1954**, *57*, 1–10.
7. Hall, A. N.; Hollingshead, S.; Rydon, H. N. *J. Chem. Soc.* **1961**, 4290–4295.
8. Dutton, G. J. *Arch. Biochem. Biophys.* **1966**, *116*, 399–405.
9. Mitchell, D. D.; Pickens, J. C.; Korotkov, K.; Fan, E.; Hol, W. G. *Bioorg. Med. Chem.* **2004**, *12*, 902–907.
10. Seidman, M.; Link, K. P. *J. Am. Chem. Soc.* **1950**, *72*, 4324.
11. Kleine, H. P.; Weinberg, D. V.; Kaufman, R. J.; Sidhu, R. S. *Carbohydr. Res.* **1985**, *142*, 333–337.
12. Matta, K. L.; Barlow, J. J. *Carbohydr. Res.* **1977**, *53*, 209–216.
13. Ishido, Y.; Shigeru, I.; Matsuno, A.; Yoshino, T.; Umezawa, H. *J. Chem. Soc., Perkin Trans. I* **1977**, 1382–1388.
14. Abboud, K. A.; Toporek, S. S.; Horenstein, B. A. *Acta Crystallogr., Sect. C.* **1997**, *53*, 118–120.
15. (a) Flack, H. D. *Acta Crystallogr., Sect. A.* **1983**, *39*, 876–881; (b) Bernardinelli, G.; Flack, H. D. *Acta Crystallogr., Sect. A* **1985**, *41*, 500–511.
16. Frisch, M. J.; Trucks, G. W.; Schlegel, H. B.; Gill, P. M. W.; Johnson, B. G.; Robb, M. A.; Cheeseman, J. R.; Keith, T.; Petersson, G. A.; Montgomery, J. A.; Raghavachari, K.; Al-Laham, M. A.; Zakrzewski, V. G.; Ortiz, J. V.; Foresman, J. B.; Cioslowski, J.; Stefanov, B. B.; Nanayakkara, A.; Challacombe, M.; Peng, C. Y.; Ayala, P. Y.; Chen, W.; Wong, M. W.; Andres, J. L.; Replogle, E. S.; Gomperts, R.; Martin, R. L.; Fox, D. J.; Binkley, J. S.; Defrees, D. J.; Baker, J.; Stewart, J. P.; Head-Gordon, M.; Gonzalez, C.; Pople J. A. Gaussian, Inc., Pittsburgh PA, 1995.
17. (a) Boese, R.; Blaser, D.; Nussbaummer, M.; Krygowski, T. M. *Struct. Chem.* **1992**, *3*, 363–368; (b) Exner, O.; Krygowski, T. M. *Chem. Soc. Rev.* **1996**, *25*, 71–75.
18. (a) Cramer, D.; Pople, J. A. *J. Am. Chem. Soc.* **1975**, *97*, 1354–1358; (b) Cramer, D. *Acta Crystallogr., Sect. B* **1984**, *40*, 498–500.
19. Żołek, T.; Paradowska, K.; Wawer, I. *Solid State NMR* **2003**, *23*, 77–87.
20. Sheldrick, G. M. Phase annealing in SHELX 90: direct methods for larger molecules. *Acta Crystallogr.* **1990**, *A46*, 467–473.
21. Sheldrick, G. M. SHELXL 93. *Program for the Refinement of Crystal Structure*; University of Göttingen: Germany, 1993.
22. *International Tables for Crystallography*; Wilson, A. J. C., Ed.; Kluwer: Dordrecht, 1992; Vol. C.